A Spontaneous Acinar Cell Carcinoma Model for Monitoring Progression of Pancreatic Lesions and Response to Treatment Through Noninvasive Bioluminescence Imaging

Ning Zhang,[1] Scott Lyons,[2] Ed Lim,[1] and Peter Lassota[1]

Abstract

Purpose: We have generated an EL1-luc/TAg transgenic mouse model that develops spontaneous and bioluminescent acinar cell carcinomas. We applied this model to noninvasively monitor tumor development and drug response.

Experimental Design: EL1-luc/TAg transgenic mice of 11 weeks of age were treated with rapamycin (5 mg/kg, i.p.) or vehicle for 6 to 12 weeks. Tumor development was monitored through bioluminescence imaging and necropsy at the study end point.

Results: EL1-luc/TAg transgenic mice showed pancreas-specific bioluminescence signal before tumor progression and produced increasing light emission from the onset of the pancreatic acinar cell carcinomas. The latency of tumor development ranged from 10 to >20 weeks of age in these mice. Progression of the primary acinar cell carcinoma was accompanied by emergence of metastatic lesions in the abdominal organs, including liver and gastrointestinal fat tissues. Rapamycin treatment suppressed tumor development.

Conclusions: The EL1-luc/TAg mouse provides a noninvasive approach for monitoring spontaneous acinar cell carcinoma development and comprises a convenient tool for the evaluation of novel therapeutics against pancreatic cancers. Tumor growth suppression through inhibition of the mammalian target of rapamycin pathway further validates this model as clinically relevant.

Pancreatic cancer is one of the leading causes of cancer deaths in the United States, with a 5-year survival from the time of diagnosis of <5% (1). The aggressiveness, the lack of effective treatments, and late detection of only advanced symptomatic pancreatic cancers due to their anatomic location behind other organs contribute to such poor outcomes (2). Lack of effective treatment for pancreatic tumors prompted development of preclinical models for evaluation of novel therapeutics. Spontaneous mouse tumor models have been used for two decades in preclinical drug development to better understand many critical components of tumor development, such as tumor-stromal interactions, the role of the immune system, metastasis, angiogenesis, and tumor cell proliferation in immunocompetent animals (3–5). Most pancreatic epithelial neoplasms recapitulate to some degree one or more of the normal cell types of the pancreas: ductal, acinar, and endocrine. Most pancreatic neoplasms (>90%) have ductal differentiation, including the most common tumor, infiltrating ductal adenocarcinoma. The small group of "nonductal" pancreatic neoplasms includes endocrine and acinar neoplasms, as well as those with mixed or undetermined differentiation (6). Spontaneous pancreatic tumor models wherein tumor development in the acinar cells of the pancreas is mediated by expression of SV40 T antigens (7, 8) or mutant Kras (9) has been previously reported. These studies increased our understanding of the molecular, physiologic, and histologic aspects of tumorigenesis. However, the use of such models in the evaluation of novel therapeutics is complicated by the variable onset of pancreatic tumor development, as well as a lack of methods to assess tumor burden without sacrificing the animal. As a result, these models usually required relatively large cohorts of animals and extensive invasive endpoint analyses to produce statistically significant drug response data.

Recent advances within the field of bioluminescence imaging have added a new tool for monitoring tumor development noninvasively in preclinical cancer models (10, 11). Bioluminescence imaging allows sensitive and rapid analysis of light emitted from luciferase-labeled cells and can be used to measure tumor burden from otherwise nonvisible deep tissue locations when caliper-based measurements are not possible. Firefly luciferase has been widely used as a bioluminescence reporter for *in vitro* and *in vivo* applications. Its activity is ATP and O_2 dependent; thus, only viable cells bioluminesce. This approach allows the researcher to noninvasively measure

Authors' Affiliations: [1]Caliper Life Sciences, Alameda, California and [2]Department of Molecular Imaging, Cancer Research UK, Cambridge Research Institute, Cambridge, United Kingdom

Received 9/2/08; revised 4/23/09; accepted 4/27/09; published OnlineFirst 7/21/09.

The costs of publication of this article were defrayed in part by the payment of page charges. This article must therefore be hereby marked *advertisement* in accordance with 18 U.S.C. Section 1734 solely to indicate this fact.

N. Zhang and S. Lyons contributed equally to this work.

Requests for reprints: Ning Zhang, Caliper Life Sciences, 2061 Challenger Drive, Alameda, CA 94501. Phone: 510-291-6157; Fax: 510-291-6232; E-mail: ning.zhang@caliperls.com.

doi:10.1158/1078-0432.CCR-08-2256

Translational Relevance

Studying development and progression of mouse tumors have proven highly useful for elucidating the mechanisms that underlie human tumor development. Consequently, murine cancer models are thought to have predictive value for clinical efficacy of experimental therapeutics. For that purpose, a noninvasive *in vivo* imaging strategy would be highly desirable for efficient therapeutic screening when tumors develop in mice in nonvisible locations. Accordingly, we have developed a transgenic mouse model (EL1-luc/TAg) wherein spontaneous and bioluminescent acinar cell carcinoma of the pancreas offers a unique opportunity for monitoring autochthonous tumor development and treatment response over time via bioluminescence imaging. Treatment with rapamycin, a suppressor of the mammalian target of rapamycin signaling pathway, inhibited the development of acinar cell carcinoma in this model. This validates the utility of this and other similar models using bioluminescence for the testing and optimization of preclinical therapeutic strategies.

relative numbers of viable cells at regular intervals following the onset of treatment. Tight correlations have been shown between photon emission and tumor burden, so the growth of primary tumors and spontaneous metastases can be quantified noninvasively, even at deep tissue sites (11, 12). Imaging studies that examine tumor response to therapeutic interventions are also able to achieve statistical significance using far smaller cohorts of experimental animals as compared with "classic" studies wherein animals had to be sacrificed at each measurement point. This can be accomplished because the tumor burden can be determined longitudinally within the same animal, and all the animals can be stratified for equal tumor burden between the groups at the beginning of the study.

Rapamycin was originally used as an antifungal agent and a suppressor of the immune system. Recently, two rapamycin analogs were shown to have clinical antitumor activity. Torisel, which has been approved, and RAD001 (Everolimus), which is currently completing phase III trials. Rapamycin and its analogs inhibit mammalian target of rapamycin (a serine/threonine kinase)–mediated signaling, which regulates cell growth, cell cycle progression, and tumorigenesis (13, 14). The inhibitory effect of rapamycin and its derivatives on *in vivo* tumor progression has been previously shown in several tumor models, including a lung adenocarcinoma with activated PI3K/Akt signaling (15), an Akt-induced mouse prostatic intraepithelial neoplasia (16), a transgenic ErbB2 mouse mammary tumor model (17), and a TgMISIIR-TAg transgenic mouse model with progression of ovarian carcinoma (18). Therapeutic efficacies of rapamycin shown in these tumor models, including T antigen–mediated ovarian carcinoma, prompted us to evaluate this drug in our EL1-luc/TAg model to illustrate its utility for testing the efficacy of mammalian target of rapamycin/PI3K/Akt pathway inhibitors as potential therapeutics.

Here, we also show for the first time that spontaneous acinar cell carcinoma development can be visualized using bioluminescence imaging. Further application of the EL1-luc/TAg acinar cell carcinoma model should enable efficient testing of the efficacy of therapeutic candidates against acinar cell carcinoma, one of the most untreatable human cancers today.

Materials and Methods

Generation of EL1-luc/TAg transgenic mouse. We used a 216-bp rat elastase 1 (EL1) promoter (19) to construct EL1-luc and EL1-TAg transgenes to confer acinar cell–specific expression of luciferase (Promega Corporation) and SV40 T and t antigens in the EL1-luc/TAg transgenic mouse. The EL1 promoter was PCR amplified from Sprague-Dawley rat genomic DNA and cloned into the pCR4Blunt-TOPO vector (Invitrogen). The EL1 promoter fragment was retrieved from the pCR4Blunt-TOPO vector as an *Eco*RI fragment and cloned into the *Sma*I site of the pGL3-Basic vector (Promega Corporation). The EL1 promoter fragment was also cloned as an *Eco*RI fragment upstream of a 2.7-kb SV40 T and t antigen sequence inside a pBlueScript vector (Stratagene Cloning Systems). The EL1-luc and EL1-TAg transgenes were used to generate transgenic mice by mixing in a 1:1 molar ratio before pronuclear microinjection of oocytes of mouse FVB/N strain (20). Both transgenes cosegregated in subsequent generations of mice. Genotyping of the transgenic mice was done primarily by imaging. The PCR amplification of a 1-kb luciferase fragment with primer pairs (forward, 5′-tggattctaaaacggattaccaggg-3′; reverse, 5′-ccaaaacaacaacggcggc-3′) was also done using mouse tail DNA.

Tissue luciferase activity. Mouse tissues were removed and homogenized in three volumes of PBS containing a protease inhibitor cocktail (Roche Applied Science) and lysed with passive lysis buffer (Promega). After centrifugation at 14,000 rpm at 4°C for 10 min, the supernatant was collected. Luciferase activity was measured by luminometer (TD-20/20, Turner Designs) using a Luciferase Assay System (Promega). Protein concentration was estimated using the Bradford assay (Sigma-Aldrich).

Bioluminescence imaging. *In vivo* imaging of luciferase activity in the pancreas was done using an IVIS imaging system (Caliper Life Sciences, formerly Xenogen Corp.). Mice were anesthetized with isoflurane and injected i.p. with 150 mg/kg of luciferin. The animals were imaged 10 min after luciferin injection. To reduce variability in measured bioluminescence resulting from variable internal placement of the pancreas, mice were imaged in three positions (ventral, left flank, and right flank). Photons emitted from the pancreas region in each position were quantified using LivingImage software, and the sum of these measurements was used as the total bioluminescence signal from the pancreas.

Rapamycin treatment. Rapamycin (LC Laboratories) was dissolved in ethanol at a concentration of 30 mg/mL and stored at -20°C. The rapamycin dosing solution was freshly prepared by diluting the rapamycin stock 1:20 with 5% polyethylene glycol–400, 5% Tween 80 solution to make a 100-μL dose (containing 0.15 mg rapamycin) for a 30-g mouse. Rapamycin was administered by i.p. injection three times weekly for the duration of the treatment. Control animals received i.p. injection of the vehicle (100 μL of 5% polyethylene glycol–400, 5% ethanol, and 5% Tween 80).

Histology. For histologic analysis, isolated tissues were immersion fixed in 4% formaldehyde (pH 7.4) overnight. The samples were then embedded in paraffin, and sections were cut for H&E staining.

Results

Generation and characterization of the EL1-Luc/TAg mouse. To create a mouse model with spontaneous pancreatic adenocarcinomas and specific labeling of the pancreas tissue with the luciferase reporter, we made two transgene constructs

(Materials and Methods) whereby the transcription of SV40 T and t antigens, and firefly luciferase were regulated by the rat EL1 promoter. After coinjection of the transgenes into the FVB/N oocytes, we obtained several transgenic founder lines. One of the founder lines was selected for this study based on specific luciferase expression in the pancreas and tumor latency roughly comparable with previously published work (21).

The EL1-luc/TAg mice were imaged with an IVIS imaging system following i.p. injection of luciferin. We initially imaged our transgenic mice in the ventral position only. However, we observed a high degree of variability in our longitudinal bioluminescent measurements, even in normal non–tumor bearing (young) animals, because of variable internal placement of the pancreas and resulting variation in the tissue depth of the light emitting cells. We found significantly less variability in our measurements when we took the sum of measured bioluminescence from right flank, left flank, and ventral positions.

Imaging analysis showed that bioluminescence was detectable from the region of the pancreas of EL1-luc/TAg mice in all positions, as expected. Male and female mice showed similar intensity in the basal bioluminescence signal (Fig. 1A). The specificity of the signal from the pancreas was further confirmed by comparing the luciferase signal from the homogenized pancreatic tissue to that from other tissues (Fig. 1B). In agreement with the *in vivo* bioluminescence imaging data, pancreatic tissue showed the highest level of luciferase activity *ex vivo*. Low levels of luciferase expression were detectable *ex vivo* in tissue homogenates of kidneys and brains of the EL1-luc/TAg mice.

Longitudinal study on acinar cell carcinoma development. Imaging of the EL1-luc/TAg mice longitudinally offers a noninvasive measure of acinar cell carcinoma progression (Fig. 2). In younger mice of 8 to 10 weeks of age, the total bioluminescence signal from the pancreas ranges from 2×10^6 to 3×10^6 photons/s. Increase of the bioluminescence signal from the baseline level to the range of 4×10^6 to 6×10^6 photons/s indicates early tumor development. The latency of tumor development varied from 10 to >20 weeks of age in these mice.

Representative mice with acinar cell carcinomas at various developmental stages, as indicated by imaging, were sacrificed for *ex vivo* imaging and for necropsy analysis. As shown in Fig. 3, a 10-week-old female mouse (Fig. 3A) has a bioluminescence signal emitted from the pancreatic region. *Ex vivo* imaging at necropsy highlighted that the predominant source of the bioluminescence was indeed the pancreas. No pancreatic tumor was observed in this mouse. In another female mouse of 12 weeks of age, an early stage of acinar cell carcinoma development was detected by imaging (Fig. 3B, *black arrows*). Necropsy analysis confirmed that small lesions had started to develop in the pancreas (Fig. 3B, *ex vivo* imaging). These areas were highly vascularized with stronger *ex vivo* bioluminescence signals. In a 19-week-old female mouse, a significant increase of the bioluminescence signal in the pancreatic and abdominal regions was observed (Fig. 3C, *left*). Necropsy analysis revealed the presence of a large acinar cell carcinoma and metastatic lesions to the liver and the mesenteric fat tissue (Fig. 3C, *right*). At late stages of tumor development in EL1-luc/TAg mice, multiple metastatic lesions to the fat tissues of the gastrointestinal tract and the reproductive organs were often detectable (Fig. 3D, *white arrows*). Metastatic tumors in the fat tissue remained bioluminescent (Fig. 3D, *middle* and *bottom right*). However, ~25% of female transgenic mice had also developed nonglowing ovarian tumors by 21 to 23 weeks of age. In the male mice, the progression of the primary acinar cell carcinoma, as well as the development of metastatic lesions, is similar to what have been observed in the female mice.

Histologic observations. We did histologic analysis of pancreas and tumor samples harvested from selected mice. The pancreas from a wild-type FVB/N mouse displaying normal histologic features is shown on Fig. 4A. Figure 4B to F shows pancreata from transgenic mice at various stages of tumor development. A small neoplastic nodule (*left*) consistent with early stage acinar cell carcinoma is shown on Fig. 4B. The rest of the pancreatic tissue showed dysplastic acini. In a large lesion displayed in Fig. 4C, the presence of pancreatic carcinoma of acinar cell origin is apparent. These carcinoma cells are highly mitotic (*black arrows*). In addition, necrosis occurred in certain areas of the tumor (*red arrows*). Figure 4D shows a poorly differentiated pancreatic carcinoma of acinar cell origin. The tumor is highly vascularized (*arrows in red color*, blood vessels),

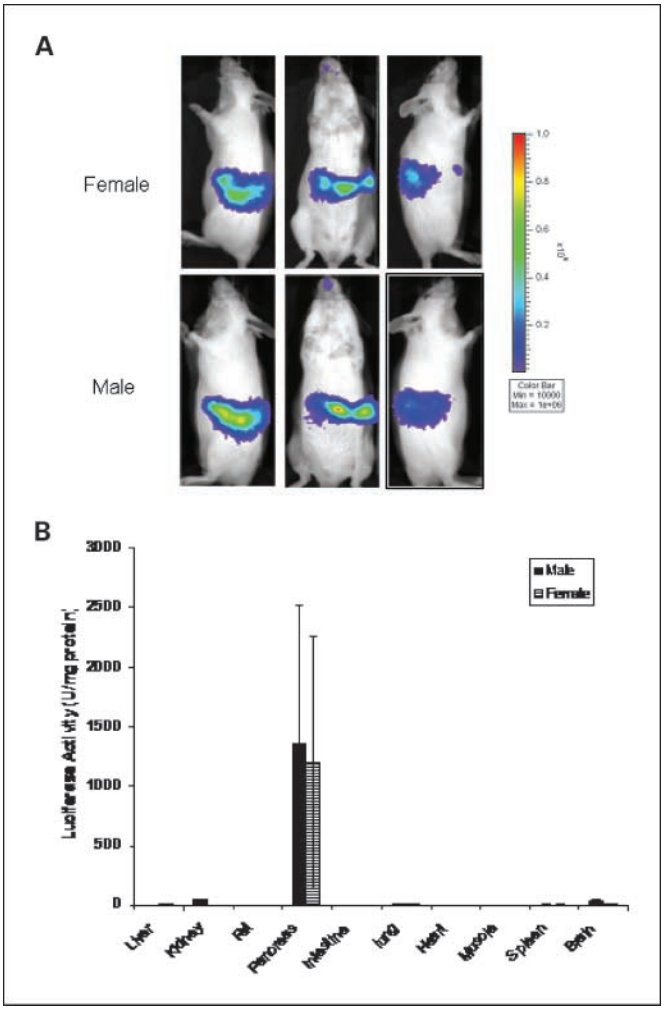

Fig. 1. *A*, EL1-luc/TAg mice of 10 wk of age were injected i.p. with luciferin and imaged with IVIS at 10 min after luciferin injection with left flank, ventral, and right flank sides of the mice facing up toward the CCD (charge-coupled device) camera. *B*, EL1-luc/TAg mice ($n = 4$) were sacrificed at 12 wk of age. Selected organs were excised, homogenized, and tested for luciferase activity. Data are presented as Mean ± SE.

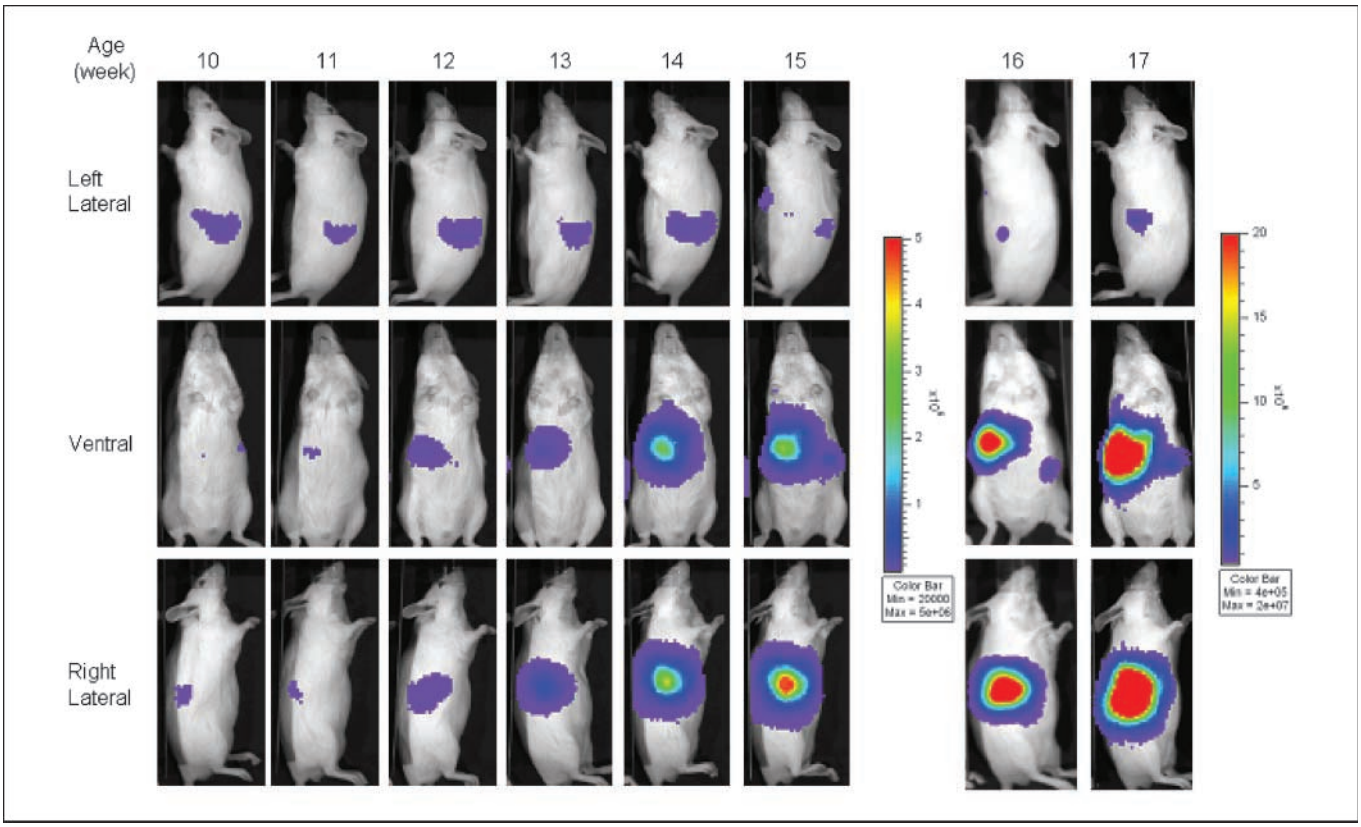

Fig. 2. A Male EL1-luc/TAg mouse was imaged twice weekly from 10 to 20 wk of age. Quantification of the signals from the pancreatic region was obtained for all three images at each time point, and the sum of all three measurements was referred to as the total pancreatic bioluminescence signal. Different scale was used for the later time points because of the dramatic increase of the bioluminescence signal.

with increased mitotic activity (*black arrows*). In some mice, liver metastases were detected. Analysis of the liver metastatic lesions showed that these small carcinomas (*arrows*) are of acinar cell origin (Fig. 4E). Many of the EL1-luc/TAg transgenic mice showed multiple metastases in the peritoneal cavity, often on the surface of the mesentery membrane. The acinar cell origin of these metastatic lesions has been confirmed by histologic examination (Fig. 4F).

Rapamycin treatment suppressed acinar cell carcinoma development in the EL1-luc/TAg mice. We tested the effect of rapamycin on acinar cell carcinoma development in the EL1-luc/TAg model. Selection of the treatment regimen was based on a previous publication (18). For this study, 24 male EL1-luc/TAg mice were used. All mice were imaged several times at the age of 9 to 10 weeks. Based on the quantification of the bioluminescence signals from the pancreas, the mice were stratified into two groups (rapamycin treated and vehicle treated, with the goal to minimize the differences in the mean light emission between the groups and the differences in light emission between the individual animals within the groups. Treatment started when the mice were 11 weeks of age. Mice in the treatment group were dosed with rapamycin thrice a week at 5 mg/kg via i.p. injections, and mice in the control group were injected with the vehicle alone for 7 weeks. Imaging was done twice a week.

Of the 24 mice used in this study, four mice (three from the rapamycin-treated group and one from the vehicle-treated group) were lost shortly after the study was initiated. The mortality of the rapamycin-treated group could be due to the adverse effects of the drug because ulceration was also observed in these mice. Initial images of a representative mouse from each group are shown in Fig. 5A. An increase of the bioluminescence signal in this vehicle-treated mouse indicated tumor development from 15 weeks of age, which was confirmed by necropsy analysis at the endpoint. The rapamycin-treated mouse showed steady basal level of luciferase signal in the pancreas region, which corresponded with the lack of tumor at necropsy. Quantification of the bioluminescence signal for each mouse is shown on Fig. 5B and C. Although most of the vehicle-treated mice showed elevation of the bioluminescence signal in time, the rapamycin-treated mice mostly showed a steady basal luciferase signal.

We did necropsy analysis at the end of the experiment (Table 1). In the male vehicle group, 8 of the 11 mice (M05, M06, M27, M31, M42, M49, M95, and M21) showed an increase of bioluminescence signal above a 30% to 40% threshold during the course of the study. Upon necropsy analysis, all these mice had developed acinar cell carcinoma in the pancreas. In addition, one mouse that showed no significant increase of the bioluminescence signal, M98, presented early stage acinar cell carcinoma development. In contrast, only two of the nine rapamycin-treated mice (M40 and M52) showed an increase of bioluminescence signal above the 30% to 40% threshold level during the imaging study. Upon necropsy analysis, both mice showed tumor development in the pancreas. Thus, the increase of bioluminescence signal in vehicle- and rapamycin-treated

mice correlated well with the presence of tumor development, as confirmed by necropsy. The pancreatic tumor mass in the vehicle-treated group ranged from <0.5 g to >1 g. Metastasis to the mesenteric fat, as indicated by *ex vivo* imaging, occurred in some of the mice (M06, M49, and M52; Table 1). Three mice from the vehicle-treated group (M42, M49, and M98) and one mouse from the rapamycin-treated group (M52) also had small metastatic tumors in the livers. Some of these metastatic tumors were no-longer glowing, possibly because of the transdifferentiation of the acinar cell carcinoma in the novel host environment.

Statistical analyses of the bioluminescence signal at the endpoint and change of the bioluminescence signal from day 0 to

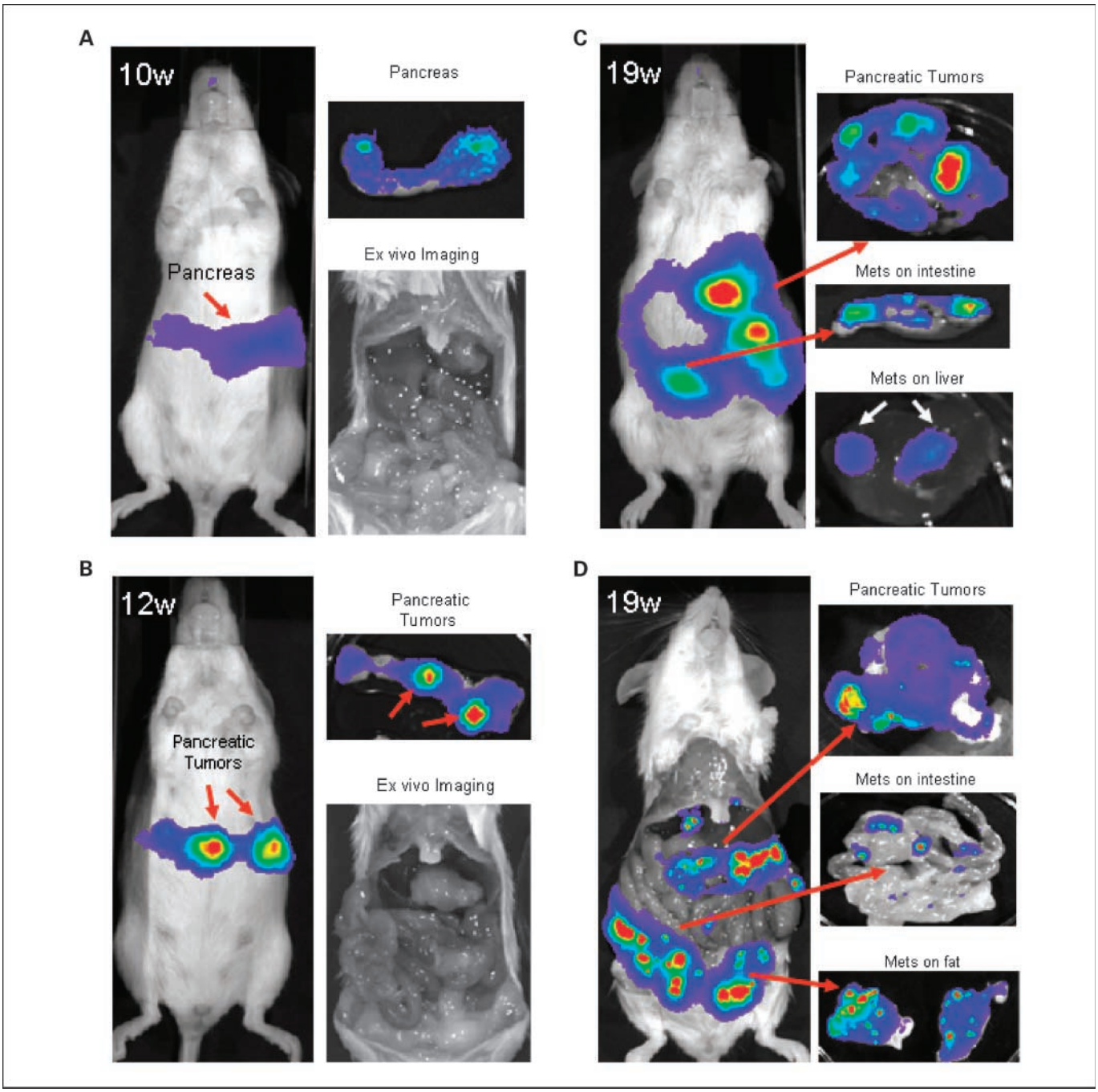

Fig. 3. *A,* bioluminescence imaging of a 10-wk-old female EL1-luc/TAg mouse showed pancreas-specific signal (*arrow*). Postmortem imaging of the excised pancreas and pancreas-free cadaver confirmed that the bioluminescence signals were restricted to the pancreas. *B,* bioluminescence imaging of a 12-wk-old female EL1-luc/TAg mouse detected increased bioluminescent signals from two hotspots (*arrows*), which represent highly vascularized small tumors (*top right*). Postmortem imaging of the pancreas-free cadaver confirms the absence of bioluminescence signal in other tissues (*bottom right*). *C,* a 19 wk-old female mouse shows significant increase of the bioluminescence signal in the pancreatic and abdominal regions. Necropsy analysis revealed a large acinar cell carcinoma in this mouse (*top right*) and metastases in the intestine (*middle right*) and liver (*bottom right*). *D,* a 19-wk-old female mouse with multiple metastases to the abdomen, as indicated by imaging (*left*). Necropsy and *ex vivo* imaging analysis showed a large tumor from the pancreas (*top right*) and metastases in mesenteric fat and reproductive fat (*middle* and *bottom right*).

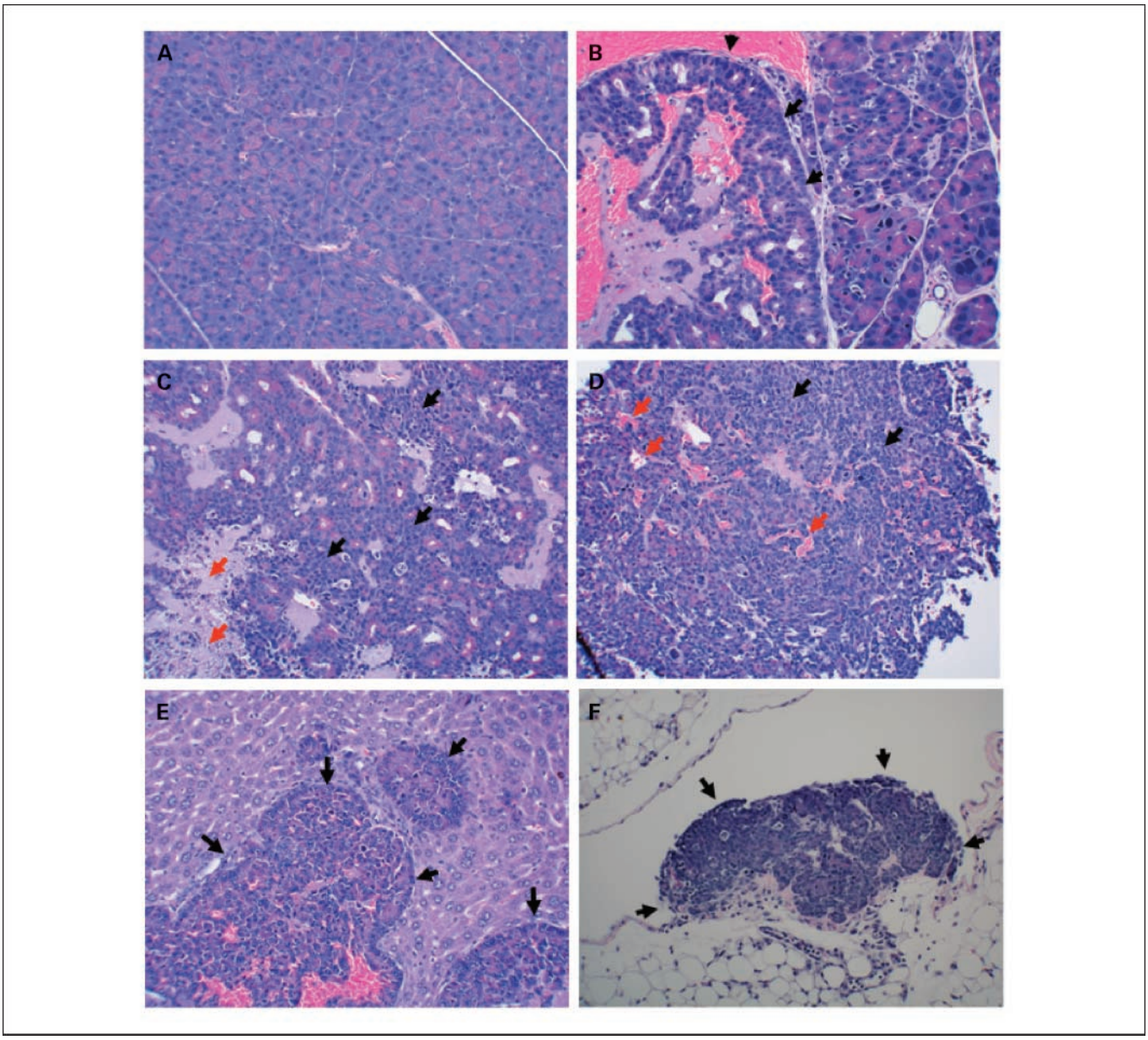

Fig. 4. Histologic analysis (H&E staining). *A,* normal pancreas. *B,* a small pancreatic carcinoma (*left, arrows*) with neoplastic nodule adjoining dysplastic pancreatic acini. *C,* a large acinar carcinoma with apparent mitotic activity and pleomorphic cell morphology. Black arrows, areas with dense nuclei and increased mitotic activity. Red arrows, necrotic areas. *D,* a poorly differentiated acinar cell carcinoma with increased mitotic activity (*black arrows*). Red arrows, blood vessels. *E,* liver metastasis (*arrows*). *F,* micrometastases on surface of mesentery membrane (*arrows*).

the endpoint (Table 1) using the Wilcoxon rank sum test were done. Both analyses showed a significant difference between the rapamycin-treated mice and the vehicle-treated controls ($P < 0.05$). In addition, analysis of the total tissue mass [pancreas plus tumor(s)] also showed a significant difference between the rapamycin-treated mice and vehicle-treated mice ($P < 0.001$).

Discussion

SV40 T antigen induces tumors in a wide variety of cell types in transgenic mice. Tissue-specific promoters controlling T-antigen expression can be used to limit tumor development to precisely defined tissues (3). Spontaneous pancreatic tumor models mediated by the expression of SV40 T antigen or Kras have previously been developed to recapitulate many key biological features of human pancreatic adenocarcinoma (7–9, 21–23). Despite the fact that SV40 T antigen is not a driver for human tumor development per se, the pathways altered, including p53 and Rb (retinoblastoma protein) tumor suppressor pathways, are relevant to human tumorigenesis (8, 19). Alterations in these tumor suppressors cause pleiotropic effects that are reflected in the deregulation of signaling pathways controlling cell proliferation, survival, adhesion, and migration (24, 25). In the past, the nonvisible nature of tumor development in the pancreas significantly limited the utility of these

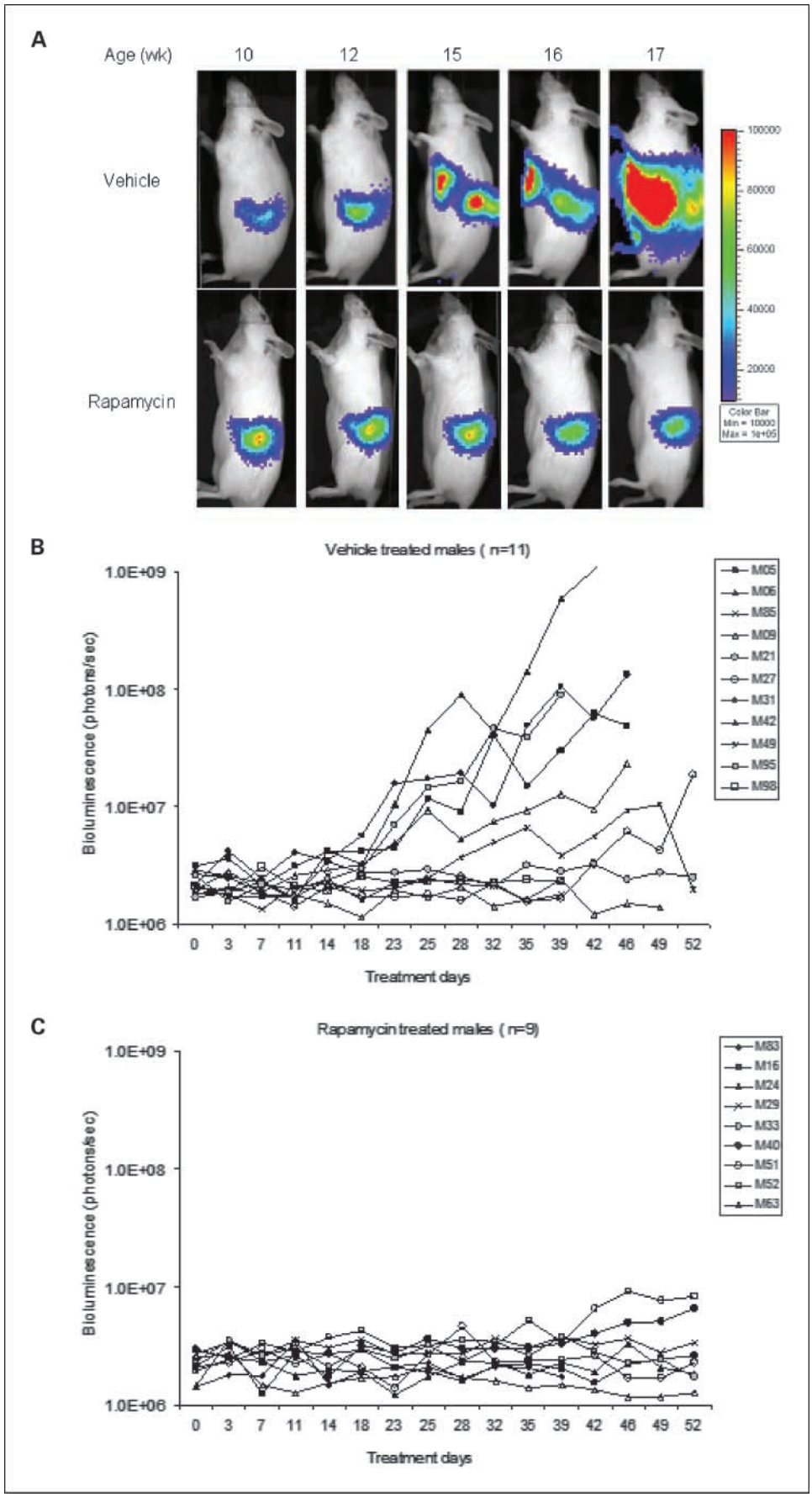

Fig. 5. Rapamycin treatment suppresses acinar cell carcinoma development. *A,* bioluminescence image of a representative mouse from rapamycin- and vehicle-treated groups. Treatment started when the mice were 11 wk of age. Longitudinal quantification analysis of bioluminescence signal of the EL1-luc/TAg mice treated with rapamycin (*B*) or with vehicle control (*C*). The units displayed on the Y axis of this graph (measured flux) correspond to the sum of measured light from three positions (ventral, right, and left flanks).

Table 1. Histologic tumor classification at necropsy and correlation of increase of bioluminescence imaging with tumor incidence

Animal ID	Treatment	BLI Day 0 ($\times 10^8$)	BLI endpoint	Change (%)	Pancreas plus tumor (g)	Acinar cell carcinoma	Metastases
M05	Vehicle	3.12×10^6	4.92×10^7	1,478 %	2.08	+	
M06	Vehicle	2.90×10^6	2.93×10^9	100,867 %	1.67	+	Metastases in fat
M85	Vehicle	1.82×10^6	1.79×10^6	-2 %	0.32		
M09	Vehicle	1.80×10^6	1.40×10^6	-22 %	N/A	N/A	
M21	Vehicle	1.69×10^6	2.49×10^6	48 %	0.31	+	
M27	Vehicle	2.67×10^6	1.88×10^7	604 %	0.3	+	
M31	Vehicle	2.18×10^6	1.33×10^8	5,983 %	5.45	+	
M42	Vehicle	1.98×10^6	2.32×10^7	1,071 %	3.67	+	Metastases in liver
M49	Vehicle	2.11×10^6	1.05×10^7	397 %	2.3	+	Metastases in liver, fat
M95	Vehicle	2.63×10^6	9.01×10^7	3,324 %	0.65	+	
M98	Vehicle	2.09×10^6	2.32×10^6	11 %	0.36		Metastases in liver
M83	Rapamycin	1.43×10^6	1.75×10^6	22 %	0.2		
M16	Rapamycin	2.15×10^6	2.63×10^6	22 %	0.23		
M24	Rapamycin	1.44×10^6	1.83×10^6	27 %	0.25		
M29	Rapamycin	2.70×10^6	3.39×10^6	25 %	0.23		
M33	Rapamycin	2.36×10^6	1.74×10^6	-26 %	0.34		
M40	Rapamycin	2.97×10^6	6.52×10^6	120 %	0.39	+	
M51	Rapamycin	2.12×10^6	2.29×10^6	8 %	0.24		
M52	Rapamycin	1.94×10^6	8.31×10^6	328 %	1.47	+	Metastases in liver, fat
M63	Rapamycin	2.50×10^6	1.27×10^6	-49 %	0.22		
Statistical significance			$P < 0.05$	$P < 0.05$	$P < 0.001$		

NOTE: EL1-luc/TAg mice treated with rapamycin or with vehicle control showed basal level of bioluminescence signal at day 0 at 11 weeks of age. Longitudinal quantification analysis of bioluminescence imaging signal is shown in Fig. 5. The endpoint data show a significant increase of bioluminescence imaging signal in M05, M06, M27, M31, M42, M49, and M95 of the vehicle-treated group and in M40 and M52 of the rapamycin-treated group. M49 was moribund at the imaging endpoint of day 52 and the bioluminescence imaging signal dropped back to basal level at that time point. Therefore, for this mouse, the endpoint bioluminescence imaging shown is from day 49. Mouse M21 showed about 100% increase of bioluminescence imaging signal from day 14 to 35, indicating tumor development occurring before the animal death. The total masses of pancreas plus tumor are shown. Mouse M09 unexpectedly died before the endpoint; therefore, the pancreas weight was not available.
Abbreviations: BLI, bioluminescence imaging; +, confirmation of the acinar cell carcinoma at necropsy; N/A, not available.

models for preclinical drug development purposes. Because bioluminescence imaging allows noninvasive assessment of luciferase labeled tumors, we established an EL1-luc/TAg mouse model to circumvent this limitation. We show here that bioluminescence imaging confers a noninvasive means to measure changes in pancreatic tumor burden in such mice. In addition, the animals can be stratified for equal tumor burden between the groups at the beginning of the study.

We used a rat EL1 promoter to drive the expression of SV40 T antigen and luciferase in the acinar cells of EL1-luc/TAg transgenic mice. In this double-transgenic mouse model, the DNA of the two transgenes was mixed before pronuclear microinjection, which usually results in the cointegration of both constructs at a single chromosomal site (26). We confirmed this by showing that the transgenes were coinherited and did not segregate in the F1 or subsequent generations following breeding of the founder mice. We generated a number of transgenic founder lines in this manner and did imaging analysis of all of them. We then selected one founder line that showed specific luciferase expression in the pancreas, as well as a tumor latency comparable with previously published work. In agreement with these previously published results (7, 8, 21), SV40 T antigen expression in the acinar cells triggered acinar cell dysplasia and acinar cell carcinomas in these mice. Expression of luciferase in the acinar cells resulted in specific emission of bioluminescence signals from the pancreas, as indicated by *in vivo* imaging and *ex vivo* analysis of various tissues from the EL1-luc/TAg mice. At the time this mouse was made, EL1 was the only well-characterized promoter that mediated exocrine cell–specific expression in the pancreas. The application of other promoters such as p48 and Pdx for mediating ductal cell–specific gene expression have since been published (27, 28). Moreover, conditional mouse models have since been developed that involve the critical players driving the development of human pancreatic cancer such as Kras, p53, and p16, and so comprise mouse models with potentially more tractable genetics than our T antigen–driven model (22, 23). In our model, we have shown for the first time the utility of bioluminescence imaging for imaging spontaneous tumors originating from the exocrine pancreas, and it should serve as a proof-of-concept for the development of future and further improved genetically engineered bioluminescent pancreatic cancer models.

Histologic analysis of the pancreas from our transgenic mice confirmed acinar cell dysplasia and neoplasia, as previously described (8, 21). The presence of acinar cell carcinoma was evident in the tissues analyzed, with a marked increase of mitotic activity in the tumor regions. Metastatic lesions observed in livers and on the surface of mesentery membranes were of acinar cell origin as well, ruling out the possibility that ectopic expression of T/t antigens in these tissues was the cause of tumor development.

Rapamycin and its derivatives have been shown to suppress tumor growth in a number of spontaneous animal tumor models, including an SV40 T antigen–mediated ovarian tumor model (18). Our data showed that rapamycin treatment significantly inhibited incidence of acinar cell carcinoma development in the EL1-luc/TAg transgenic mice and that tumor development could be monitored noninvasively using bioluminescence imaging. Some of the rapamycin-treated mice escaped the effect of this mammalian target of rapamycin inhibitor. It is possible that T antigen–mediated oncogenesis activated many different pathways that contribute to cell proliferation and that certain pathways in the rapamycin-resistant tumor could compensate for the inhibition of the mammalian target of rapamycin pathway resulting from rapamycin treatment. Obviously, identifying these pathways will help design therapeutic strategies that circumvent resistance to mammalian target of rapamycin inhibitors.

When doing bioluminescence imaging, there are several factors that can contribute to variation of the luciferase signal. There factors include the quality of i.p. delivery of luciferin, the difference of Luciferin distribution kinetics, and timing of imaging acquisition. As a result, a difference of 30% to 40% of the luciferase activity could be caused by these variables. When doing data analysis, it is necessary to review all the data longitudinally. Luciferase signal that is consistently above a 30% to 40% threshold should be regarded as an increase of luciferase expression per se. The converse is also true when luciferase signal declines during the study.

Development of acinar cell carcinoma was accompanied by metastases in mesenteric fat associated with the digestive tract and in liver tissues in some mice. Although metastases to the mesenteric fat are detectable with *in vivo* imaging, we were unable to definitely locate liver metastases because of the fact that not all of the liver metastases were glowing, as revealed by *ex vivo* imaging. This could be due to the dramatic change of tissue environment surrounding cancer cells, which may have caused transdifferentiation of the acinar cell carcinoma in the liver and inactivation of the EL1 promoter activity, which controls luciferase expression.

We have also examined the female EL1-luc/TAg mice for pancreatic tumor development. Similar to the male mice, development of acinar cell carcinoma and metastases in livers and fat was observed. In addition, we observed nonglowing ovarian tumors in a number of rapamycin-treated female mice that did not have acinar cell carcinoma in the pancreas (data not shown). Histologic analysis also showed that the ovarian tumor originated from the ovary, not from the pancreas. Thus, the development of ovarian tumors slightly complicates the use of female mice for future applied *in vivo* studies, and so male EL1-luc/TAg mice will be preferred for future drug screening applications.

In summary, we have established a spontaneous tumor model for tracking acinar cell carcinoma development noninvasively and longitudinally with bioluminescence imaging. Treatment of these mice with rapamycin significantly inhibited tumor development, as indicated by bioluminescence imaging and necropsy analysis. This study provides evidence of a positive drug response of acinar cell carcinomas in the male EL1-luc/TAg mice. Further utility of this model will be in preclinical drug development of other agents against acinar cell carcinomas. The clinical complexity of human pancreatic tumorigenesis and the poor prognosis after detection currently makes pancreatic cancer an incurable disease. The establishment of additional animal models that better recapitulate clinical pancreatic tumor development is necessary for the effective preclinical evaluation of novel therapeutics against pancreatic cancer.

Disclosure of Potential Conflicts of Interest

No potential conflicts of interest were disclosed.

Acknowledgments

We thank Drs. Ken Campbell, Richard Coffee, and David Grass in generating transgenic mouse founder lines; and Michael Vigil, Rhonda Gregory, and Margaret Cobos for animal husbandry.

References

1. Moore PS, Beghelli S, Zamboni G, Scarpa A. Genetic abnormalities in pancreatic cancer. Mol Cancer 2003;2:7.
2. Landies SH, Murray T, Bolden S, Wingo PA. Cancer statistics. J Am Cancer Soc 1999;49:8–31.
3. Hanahan D. Transgenic mice as probes into complex systems. Science 1989;246:1265–75.
4. Bergers G, Javaherian K, Lo KM, Folkman J, Hanahan D. Effects of angiogenesis inhibitors on multistage carcinogenesis in mice. Science 1999;284:808–12.
5. Frese KK, Tuveson DA. Maximizing mouse cancer models. Nat Rev Cancer 2007;7:645–58.
6. Klimstra DS. Nonductal neoplasms of the pancreas. Mod Pathol 2007;20 Suppl 1:S94–112.
7. Longnecker DS, Kuhlmann ET, Freeman DH, Jr. Characterization of the elastase 1-simian virus 40 T-antigen mouse model of pancreatic carcinoma: effects of sex and diet. Cancer Res 1990; 50:7552–4.
8. Tevethia MJ, Bonneau RH, Griffith JW, Mylin L. A simian virus 40 large T-antigen segment containing amino acids 1 to 127 and expressed under the control of the rat elastase-1 promoter produces pancreatic acinar carcinomas in transgenic mice. J Virol 1997; 71:8157–66.
9. Grippo PJ, Nowlin PS, Demeure MJ, Longnecker DS, Sandgren EP. Preinvasive pancreatic neoplasia of ductal phenotype induced by acinar cell targeting of mutant Kras in transgenic mice. Cancer Res 2003;63:2016–9.
10. Contag CH, Spilman SD, Contag PR, et al. Visualizing gene expression in living mammals using a bioluminescent reporter. Photochem Photobiol 1997;66:523–31.
11. Lyons SK, Lim E, Clermont AO, et al. Noninvasive bioluminescence imaging of normal and spontaneously transformed prostate tissue in mice. Cancer Res 2006;66:4701–7.
12. Lyons SK. Advances in imaging mouse tumour models *in vivo*. J Pathol 2005;205:194–205.
13. Bjornsti MA, Houghton PJ. The TOR pathway: a target for cancer therapy. Nat Rev Cancer 2004; 4:335–48.
14. Hidalgo M, Rowinsky EK. The rapamycin-sensitive signal transduction pathway as a target for cancer therapy. Oncogene 2000;19:6680–6.
15. Wislez M, Spencer ML, Izzo JG, et al. Inhibition of mammalian target of rapamycin reverses alveolar epithelial neoplasia induced by oncogenic K-ras. Cancer Res 2005;65:3226–35.
16. Majumder PK, Febbo PG, Bikoff R, et al. mTOR inhibition reverses Akt-dependent prostate intraepithelial neoplasia through regulation of apoptotic and HIF-1-dependent pathways. Nat Med 2004;10:594–601.
17. Liu M, Howes A, Lesperance J, et al. Antitumor activity of rapamycin in a transgenic mouse model of ErbB2-dependent human breast cancer. Cancer Res 2005;65:5325–36.
18. Mabuchi S, Altomare DA, Connolly DC, et al. RAD001 (Everolimus) delays tumor onset and progression in a transgenic mouse model of ovarian cancer. Cancer Res 2007;67:2408–13.
19. Ornitz DM, Hammer RE, Messing A, Palmiter RD, Brinster RL. Pancreatic neoplasia induced by SV40 T-antigen expression in acinar cells of transgenic mice. Science 1987;238:188–93.

20. Hogan B. Manipulating the mouse embryo: a laboratory manual. 2nd ed. p. xvii, 497Cold Spring Harbor (NY): Cold Spring Harbor Laboratory Press; 1994.
21. Fowlis DJ, Balmain A. Oncogenes and tumour suppressor genes in transgenic mouse models of neoplasia. Eur J Cancer 1993;29A:638–45.
22. Schneider G, Siveke JT, Eckel F, Schmid RM. Pancreatic cancer: basic and clinical aspects. Gastroenterology 2005;128:1606–25.
23. Prasad NB, Biankin AV, Fukushima N, et al. Gene expression profiles in pancreatic intraepithelial neoplasia reflect the effects of Hedgehog signaling on pancreatic ductal epithelial cells. Cancer Res 2005;65:1619–26.
24. Vooijs M, Jonkers J, Lyons S, Berns A. Noninvasive imaging of spontaneous retinoblastoma pathway-dependent tumors in mice. Cancer Res 2002;62:1862–7.
25. Zhu L, Shi G, Schmidt CM, Hruban RH, Konieczny SF. Acinar cells contribute to the molecular heterogeneity of pancreatic intraepithelial neoplasia. Am J Pathol 2007;171:263–73.
26. Warner SL, Muñoz RM, Bearss DJ, Grippo P, Han H, Von Hoff DD. Pdx-1-driven overexpression of aurora a kinase induces mild ductal dysplasia of pancreatic ducts near islets in transgenic mice. Pancreas 2008;37:e39–44.
27. Hingorani SR, Petricoin EF, Maitra A, et al. Preinvasive and invasive ductal pancreatic cancer and its early detection in the mouse. Cancer Cell 2003;4:437–50.
28. Aguirre AJ, Bardeesy N, Sinha M, et al. Activated Kras and Ink4a/Arf deficiency cooperate to produce metastatic pancreatic ductal adenocarcinoma. Genes Dev 2003;17:3112–26.